

Microcracking Indicators predict Shear Failure in Berea Sandstone

Insights using the Discrete Element Method and Machine Learning

Harsh Biren Vora, Julia Morgan

Department of Earth Science, Rice University, Houston, TX, 77006



RICE

Abstract

We investigate possible indicators of critical point behavior prior to rock failure using statistical properties of microcracking during failure of rocks under differential compression. We conduct a multivariate, temporal analysis of microcracking rate and mode, fracture energy release, seismic moment and fractal distribution of deformation. Our results reveal several critical point indicators, each behaving as a time-to-failure function. The calculated precursory signatures are used as input for a feedforward Neural Network to predict rock failure. Our tool shows strong stress-to-failure ($R=0.99$) and strain-to-failure ($R=0.96$) prediction capabilities.

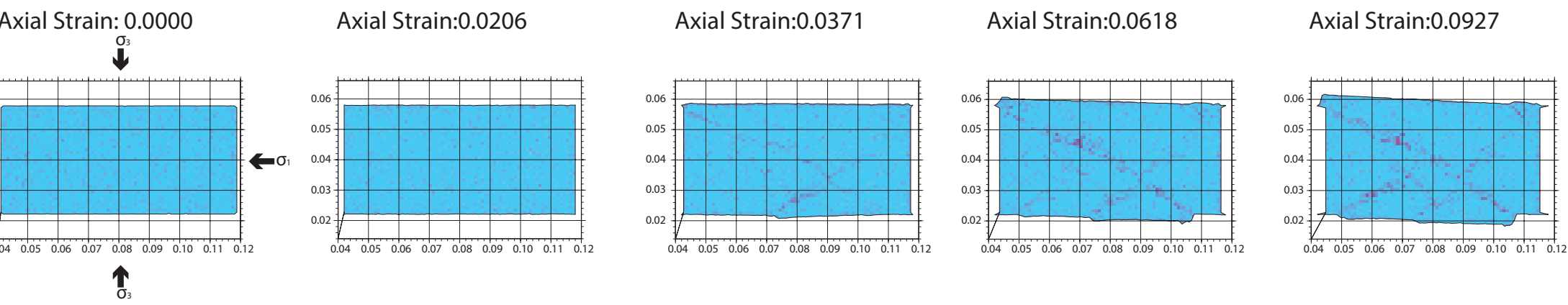
Discrete Element Method

- Construct geologic medium as assemblage of simple particles – disks or spheres
 - Apply physical properties to particles: Contact friction, elastic properties
 - Implement interparticle bonds to simulate cohesion, which can fail under normal, shear, and rotational stresses
 - Resolve forces onto particles and track resultant motion
- Confining Laws:** $f_n = f_n(\theta, \dot{\theta})$, $f_s = f_s(\theta, \dot{\theta})$, $F_p = m \cdot a$.
Newton's Equation of Motion: $\ddot{r} = F_p - \sum f_i$.
Force – Normal Displacement Relationships: $f_n = f_n(\theta, \dot{\theta}, Q)$, $f_s = f_s(\theta, \dot{\theta}, Q)$.
Shear Force – Normal Force Failure Criteria: $f_s > 0, f_n < \mu \cdot f_s + C_0$, $f_n > 0, f_n < C_0(1 - f_s/f_{s,\max})$, $f_s < \mu \cdot f_n$.

Model Setup and Methods

1. Setup biaxial experimental setup

- Domain size: 0.12m x 0.06 m
- 3240 particles with radius of 300 μm
- 2700 particles with radius of 400 μm
- Preconsolidate each sample to 10 MPa



2. Simulate Biaxial Experiments under 0 - 50 MPa Confining Pressure

3. Calibrate Bulk Geomechanical Properties of Berea Sandstone

- Unconfined Compressive Strength = 85 MPa
- Young's Modulus = 6.1 GPa
- Mohr-Coulomb Cohesion = 29.3 MPa
- Mohr-Coulomb Slope = 29°

Young's Modulus of Bonds	5 x 10 ¹⁰ Pa
Shear Modulus of Bonds	5 x 10 ¹⁰ Pa
Tensile Strength of Bonds	9 x 10 ¹⁰ Pa
Cohesion of Bonds	9 x 10 ¹⁰ Pa
Poisson's Ratio of Particles	0.33

4. Quantify Fracture Energy From Microcracking

$$E_f = (\frac{1}{2})^n (C_f)^2 V_f / C_t$$

E_f : Energy of microcrack
 C_f : Elastic Modulus of interparticle bond
 σ_{cf} : Failure Stress of interparticle bond
 V_f : Volume of Microcrack

5. Implement Spatio-Temporal Clustering to calculate Seismic Moment

$$M_e = (\frac{1}{2}) \log_{10} E_f - 2.9$$

M_e : Seismic moment

$$\log N(M_e) = a - bM$$

N : Number of events with magnitude greater than M

b : Slope of Frequency-Magnitude curve

6. Quantify Microcrack distribution using Fractal D-value

$$C(R) = 2N_{(r=R)} / N(N-1)$$

$$C(R) \propto R^D$$

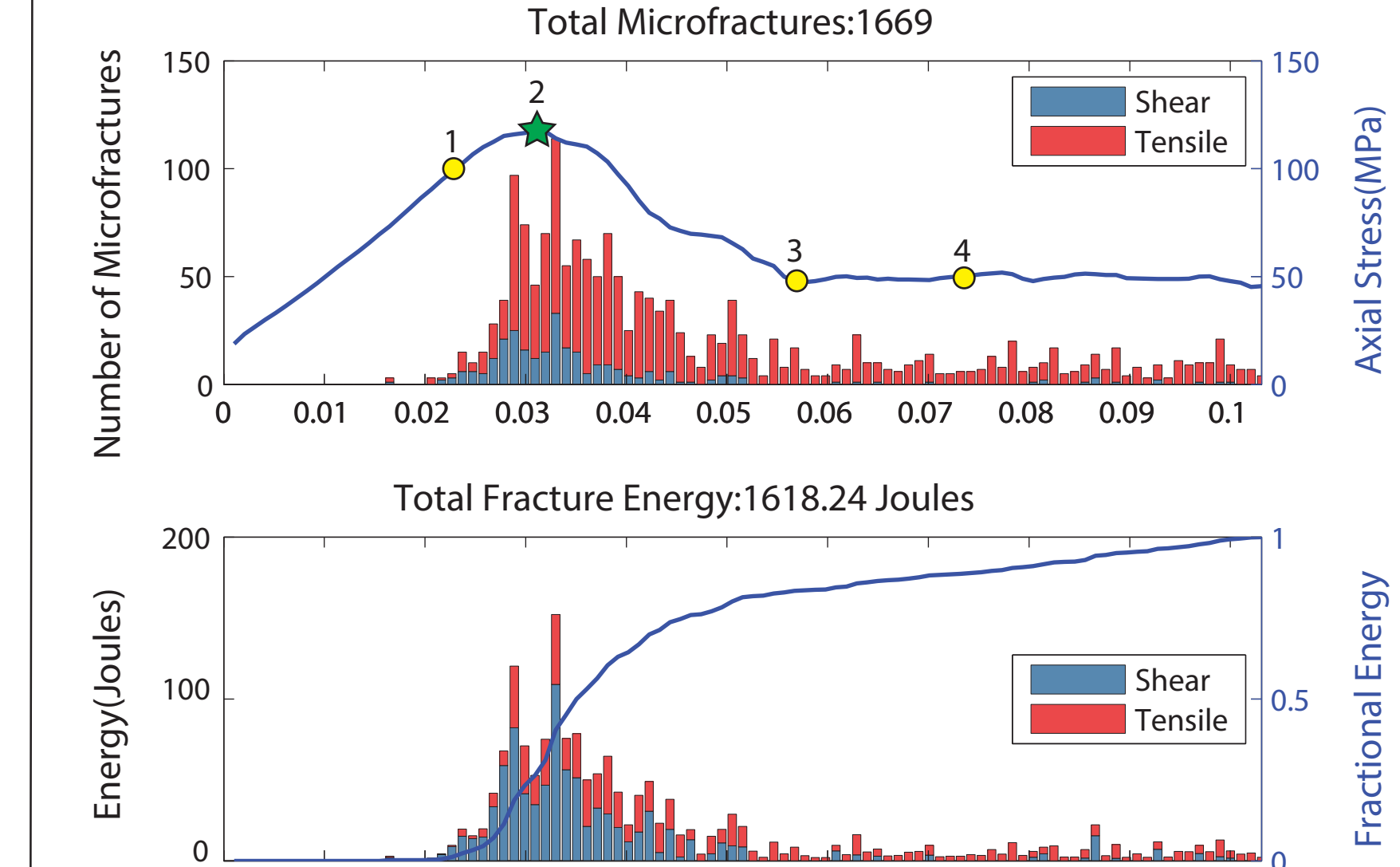
D : Fractal Dimension
N : Number of microcrack pairs
R : Radial distance (m)

Low D-values: Localized microcracking
High D-value: Distributed microcracking

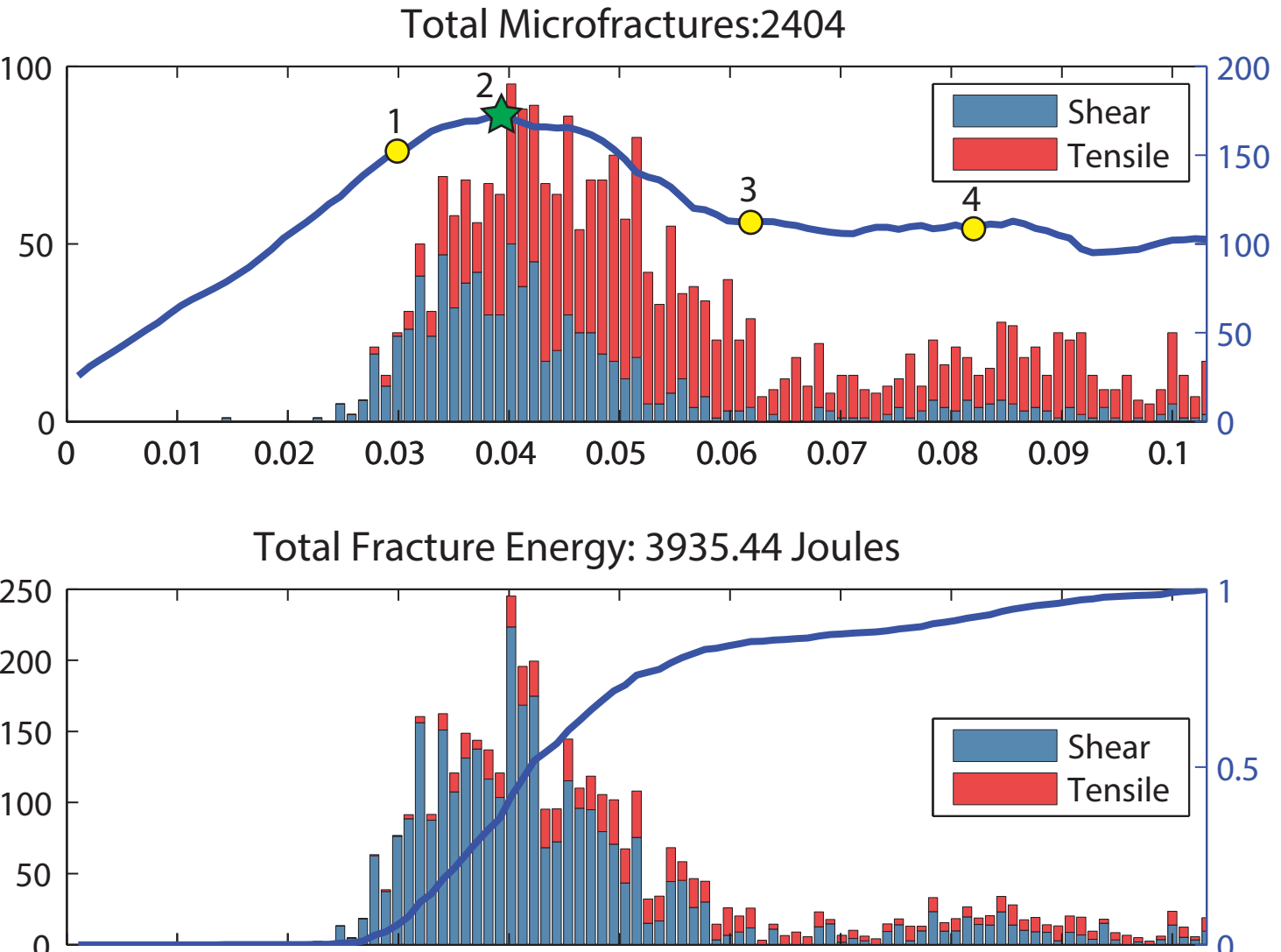
Shear Fracture Growth in Berea Sandstone

We calculate statistical variations in rate, mode, energy and moment associated with microcracking during confined biaxial experiments simulated upon numerical analogs of Berea Sandstone

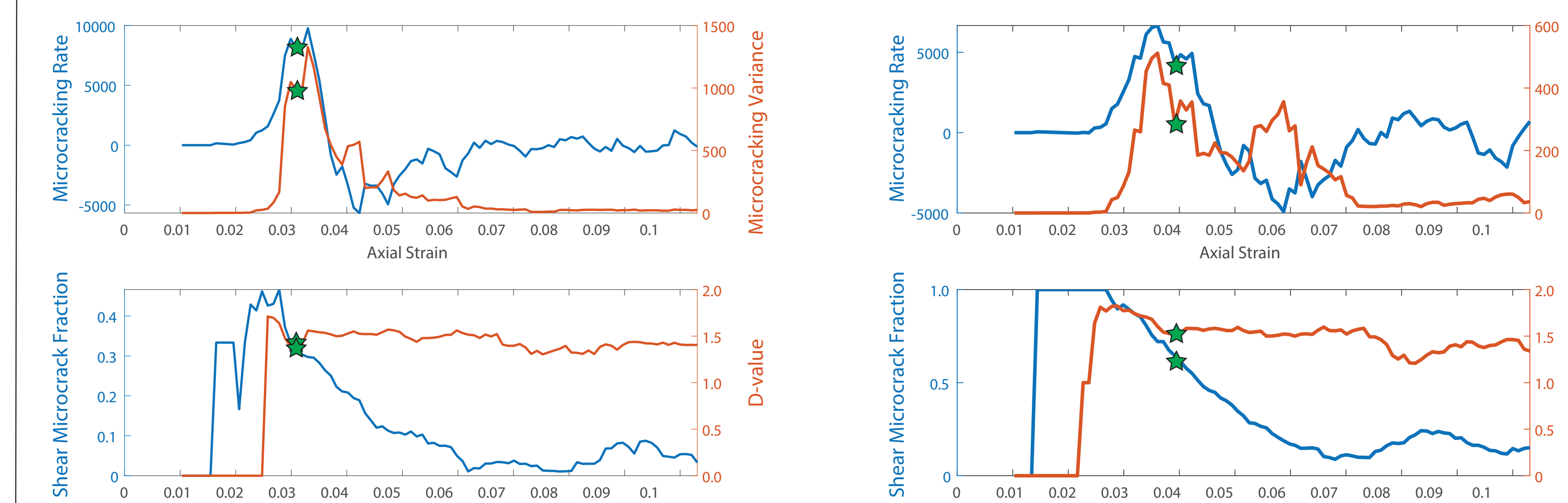
Confining Pressure = 10 MPa



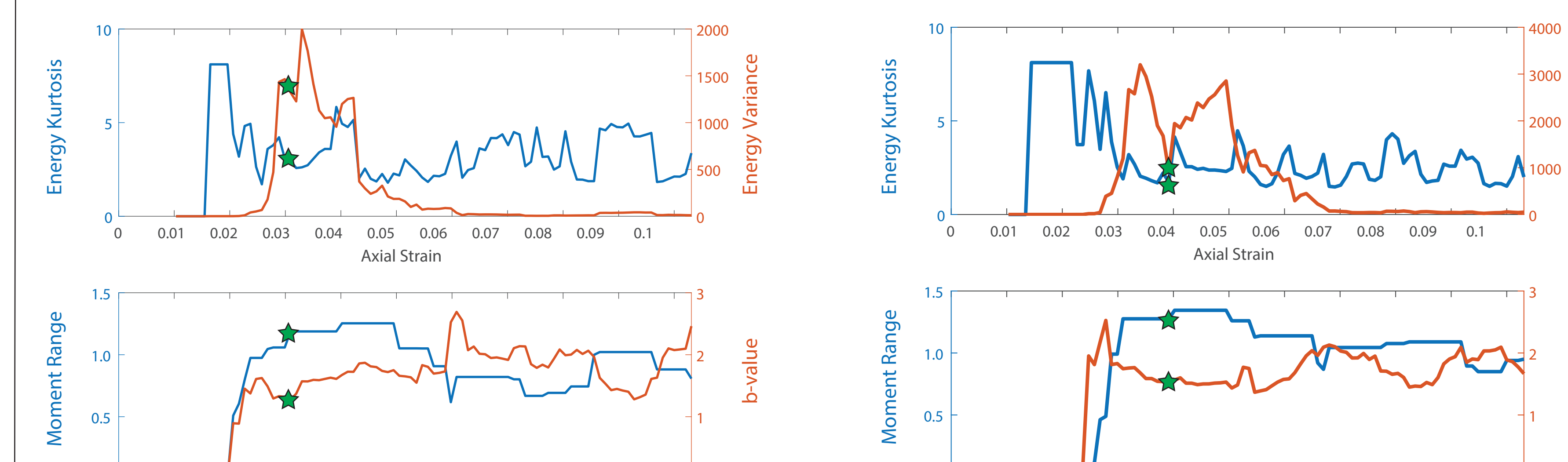
Confining Pressure = 35 MPa



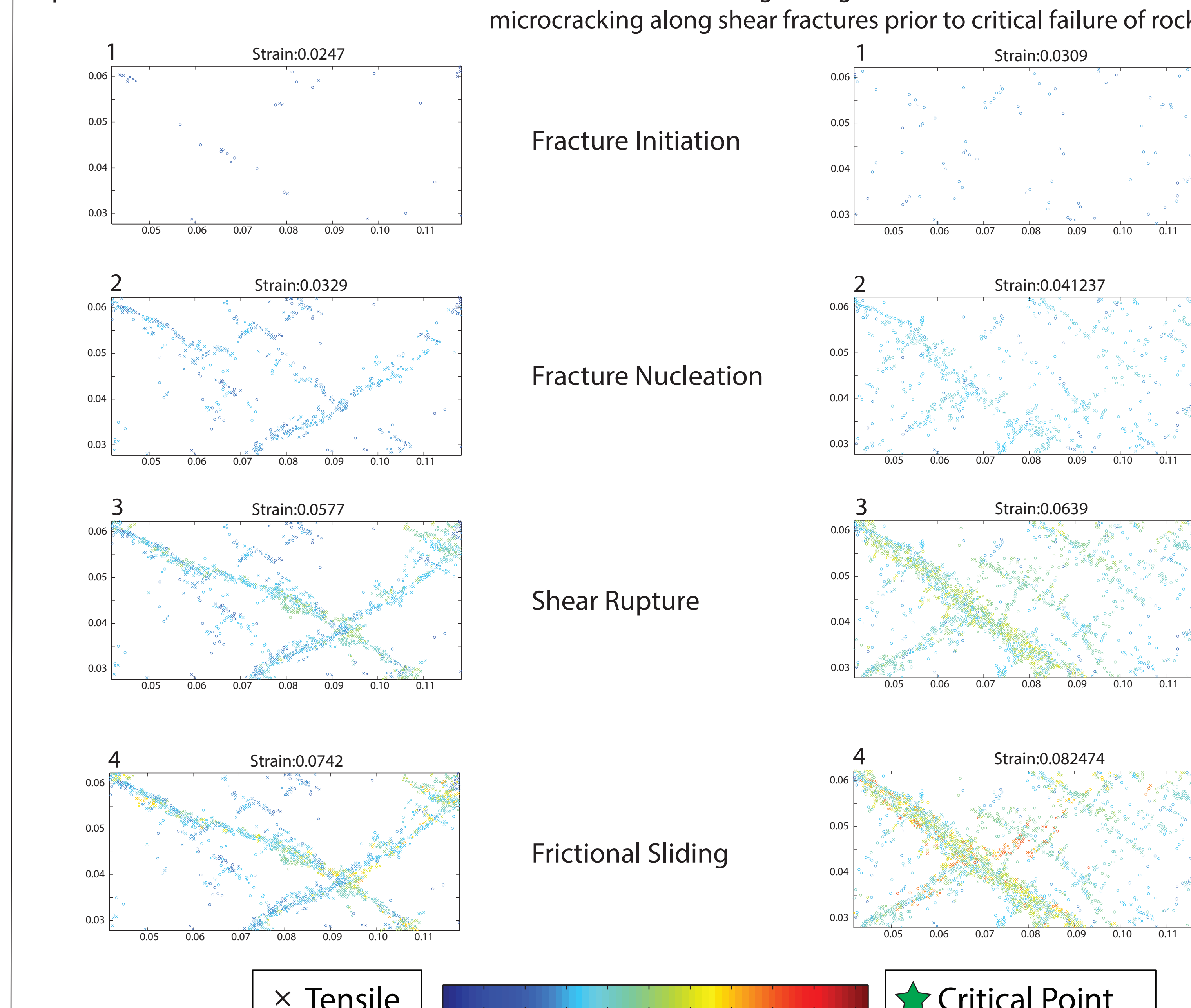
Microcracking Rate: Critical Failure is preceded by an increase in Microcracking Rate and Variance, and increase in Shear microcrack fraction



Fracture Energy and Seismic Moment: Critical Failure is preceded by an increase in Energy Variance and decline in seismic b-values



Spatial Distribution of Microcracks: Distributed microcracking during Fracture Initiation transitions into localized microcracking along shear fractures prior to critical failure of rock



References

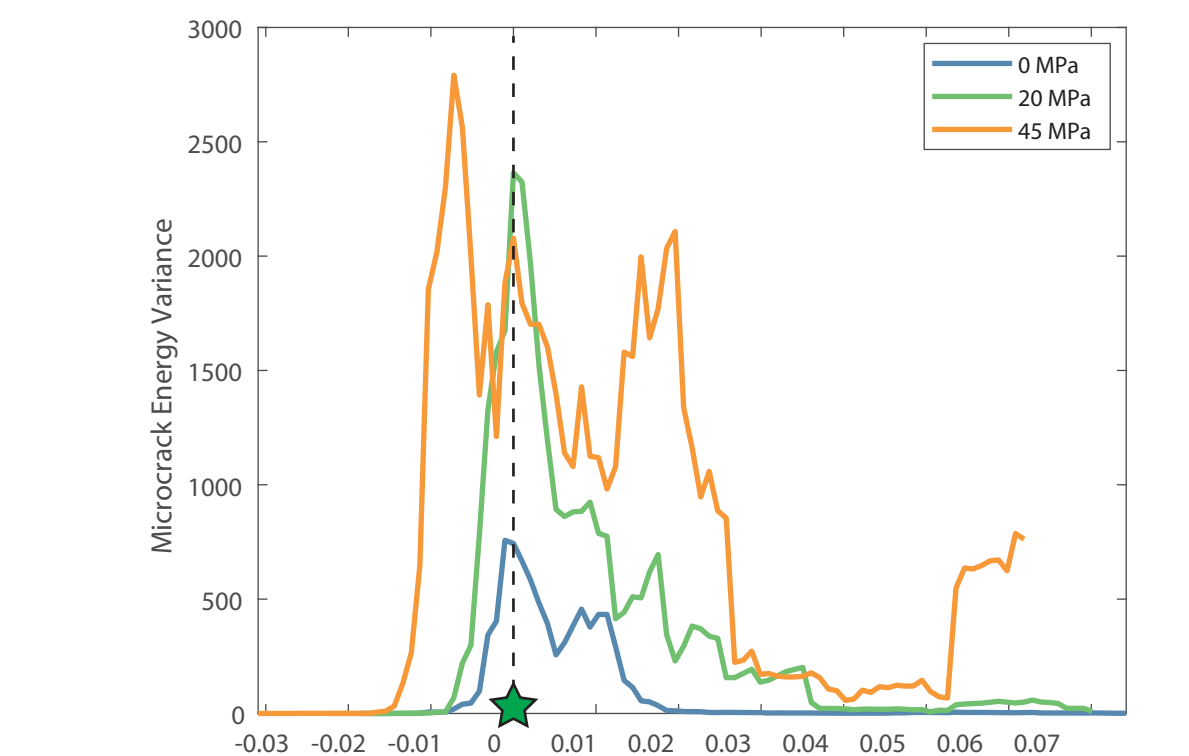
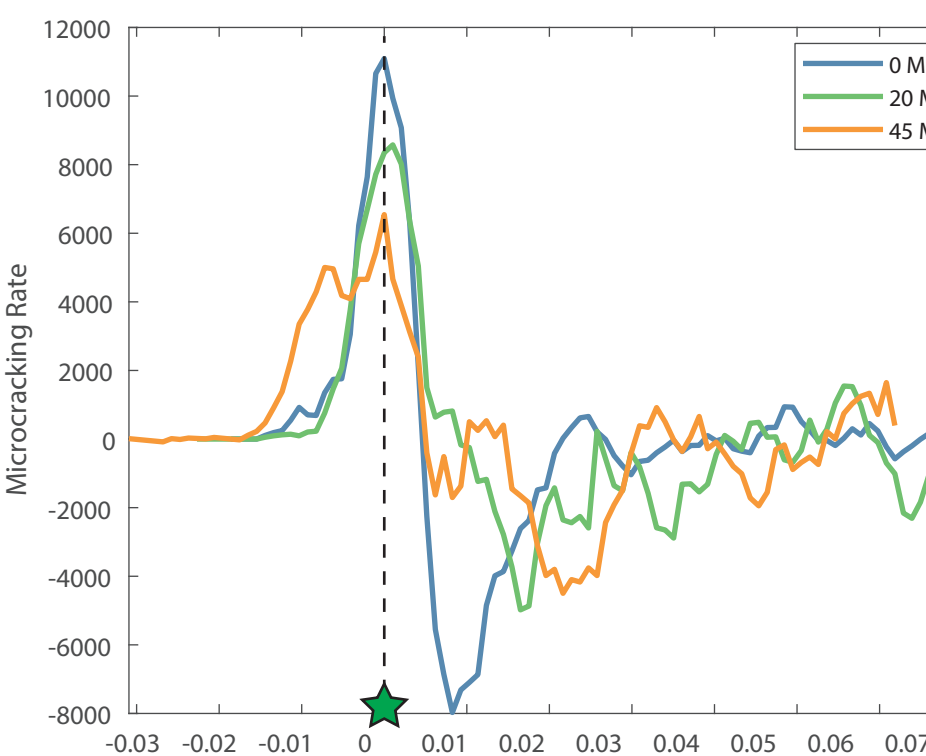
- Lei, X., and Schedl, T., 2007. Indication of critical point behavior prior to rock failure inferred from pre-failure damage. *Tectonophysics*, 431(1–4), pp.97–111.
- Rouet-Loisel, B., Hubert, C., Lubien, N., Barros, K., Humphreys, C.J., and Johnson, P.A., 2017. Machine learning predicts laboratory earthquakes. *Geophysical Research Letters*, 44(18), pp.9276–9282.
- Tang, C.A., and Kaiser, P.K., 1998. Numerical simulation of cumulative damage and seismic energy release during brittle rock failure—part I: fundamentals. *International Journal of Rock Mechanics and Mining Sciences*, 35(2), pp.113–121.
- Hazard, J.F., 2000. Simulating Acoustic Emission in bonded-particle models of rock. *Int. J. Rock Mech. Min. Sci.*, 37(5), pp.867–872.
- Morgan, J.K., 2015. Effects of cohesion on the structural and mechanical evolution of fold and thrust belts and contractional wedges: Discrete element simulations. *Journal of Geophysical Research: Solid Earth*, 120(5), 3870–3896.
- Lockner, D., 1993, December. The role of acoustic emission in the study of rock fracture. In: *International Journal of Rock Mechanics and Mining Sciences & Geomechanics Abstracts* (Vol. 30, No. 7, pp. 883–899). Pergamon.
- Scholte, L., and Donze, F.V., 2013. A DEM model for soft and hard rocks: role of grain interlocking on strength. *Journal of the Mechanics and Physics of Solids*, 61(2), 352–369.

Precursory Signatures of Rock Failure

We identify the following indicators of critical point behavior prior to rock failure :

1. Microcracking

- Increase in microcracking rate
- Increase in microcracking variance
- Increase in Shear microcrack fraction



2. Fracture Energy

- Increase in Energy Variance
- Decline in Energy Kurtosis

3. Seismic Moment:

- Increase in Moment Range
- Decline in b-value

4. Spatial distribution of microcracks:

- Decline in D-value

Critical Failure Prediction

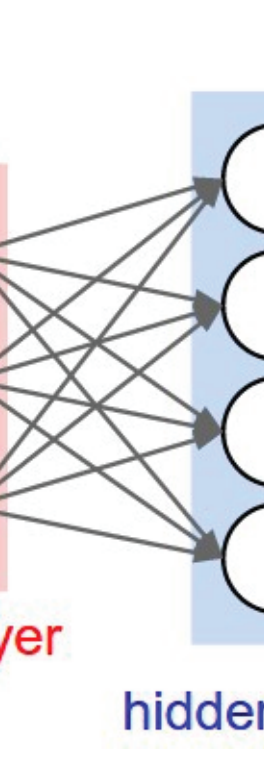
We employ a feedforward Neural Network to Predict rock failure in Berea Sandstone using calculated precursory indicators of critical point behavior

Inputs:

- Microcrack Rate
- Microcrack Variance
- Shear Microcrack Fraction
- Microcrack Energy Variance
- Microcrack Energy Kurtosis
- Seismic Moment Range
- Seismic b-value
- Fractal Dimension (D-value)
- Confining Pressure on sample

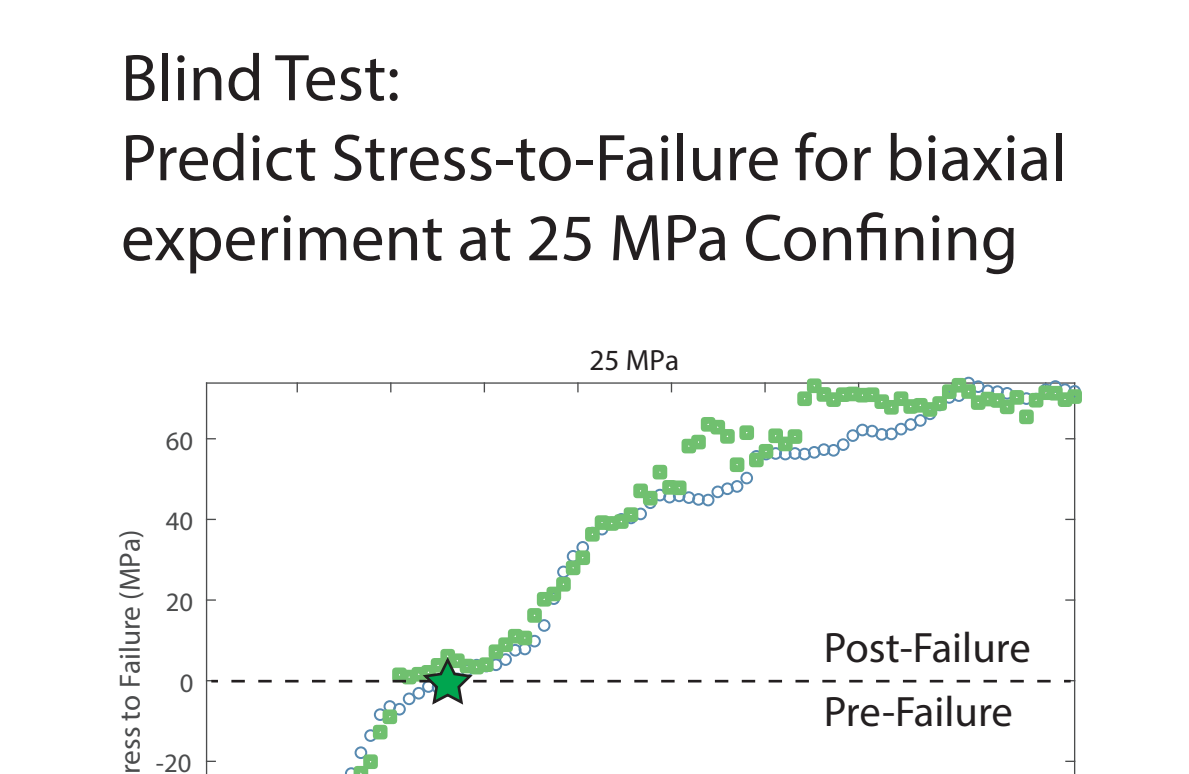
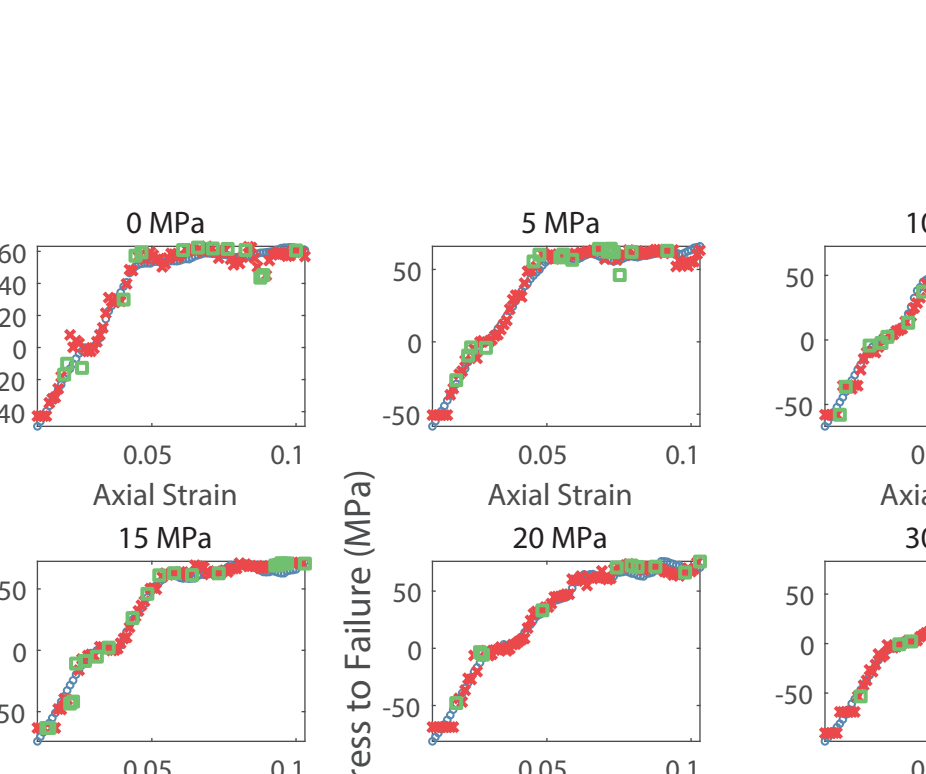
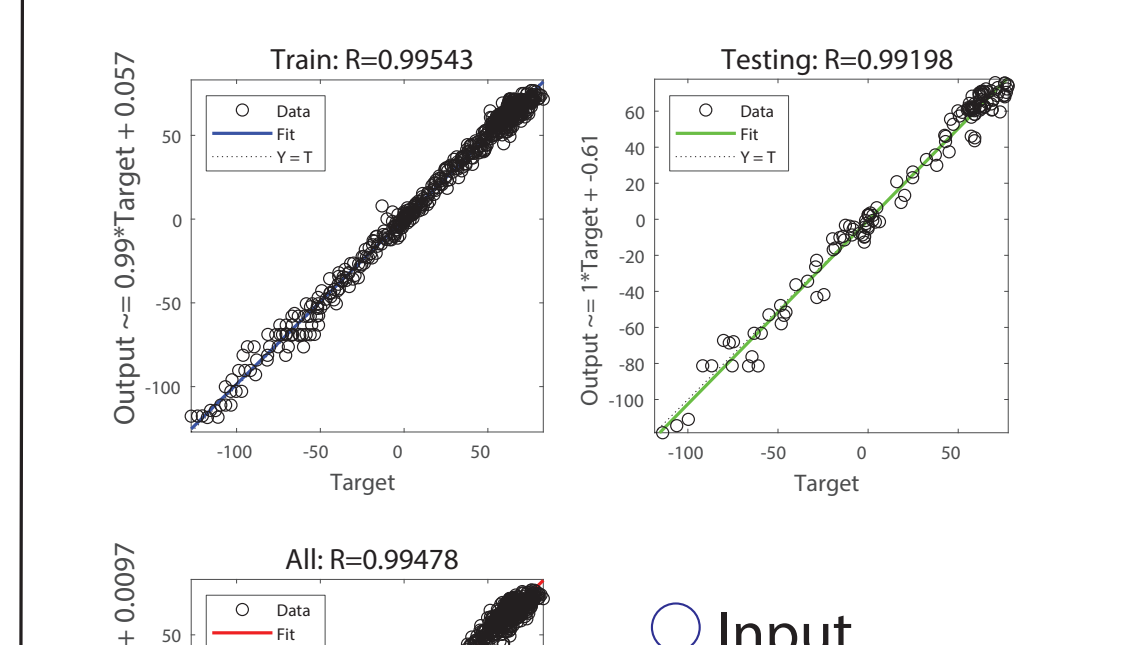
Outputs:

- Axial Stress to Failure
- Axial Strain to Failure

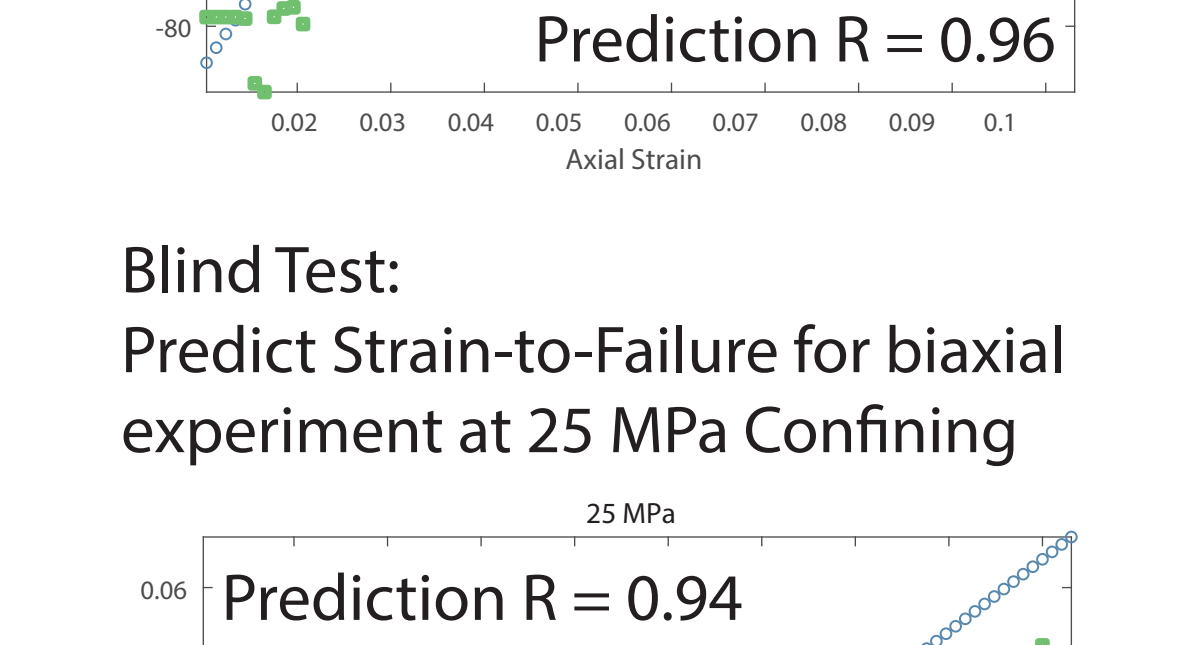
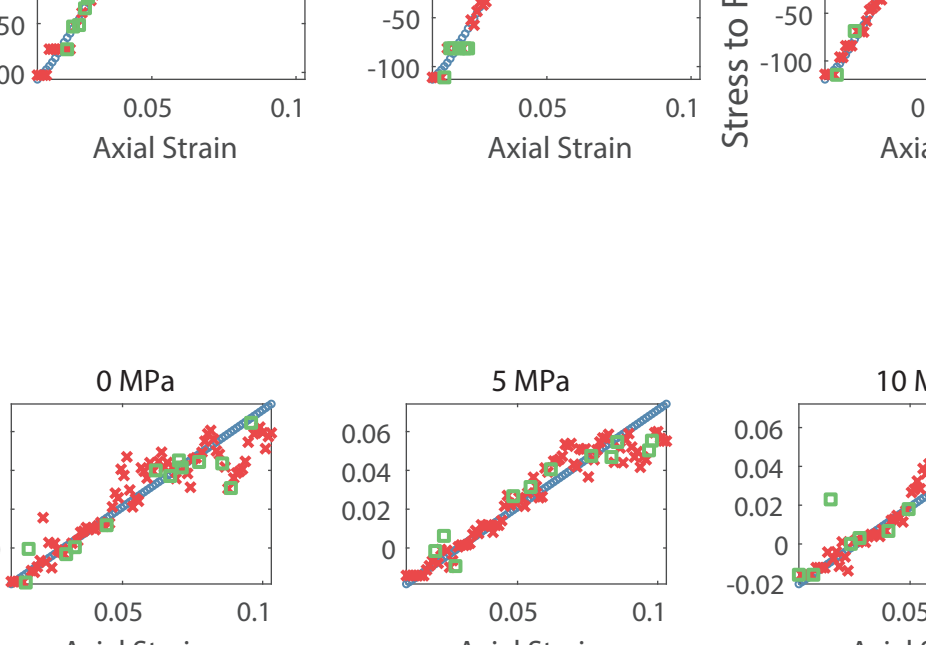
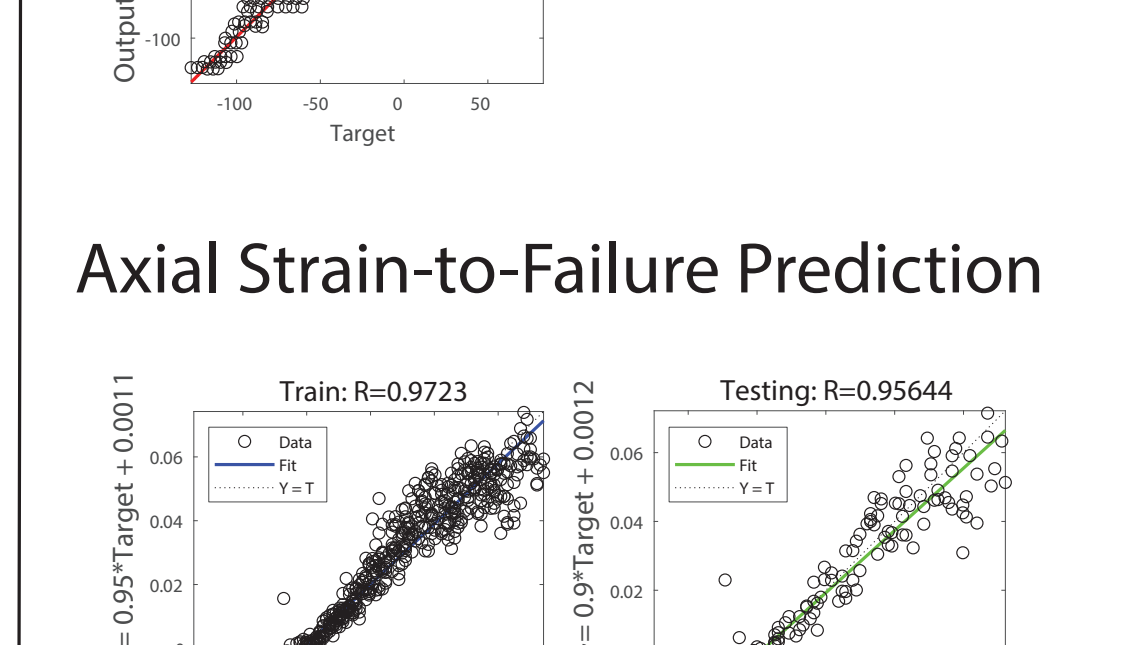


Input Dataset: 910 (datasteps) x 9 (parameters)
Number of Hidden Layers: 1
Neurons in Hidden Layer: 9

Axial Stress-to-Failure Prediction

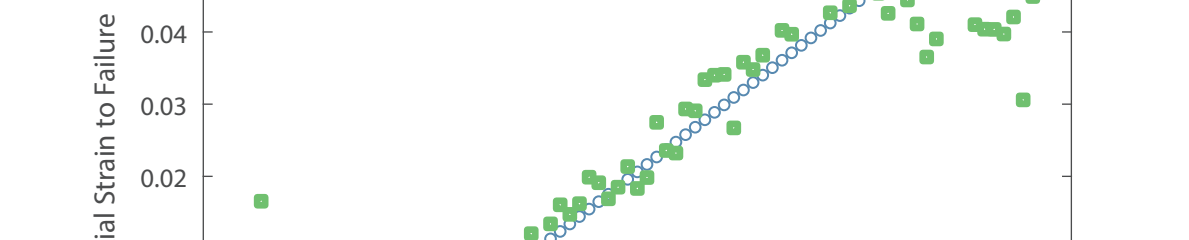
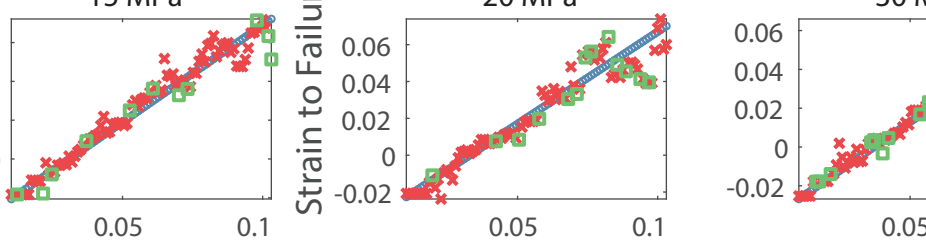


Axial Strain-to-Failure Prediction



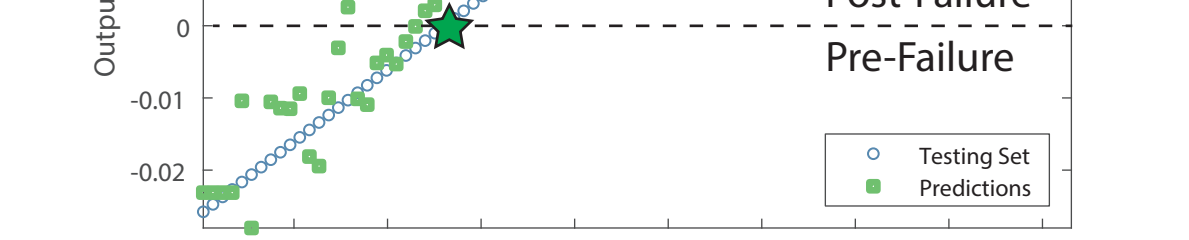
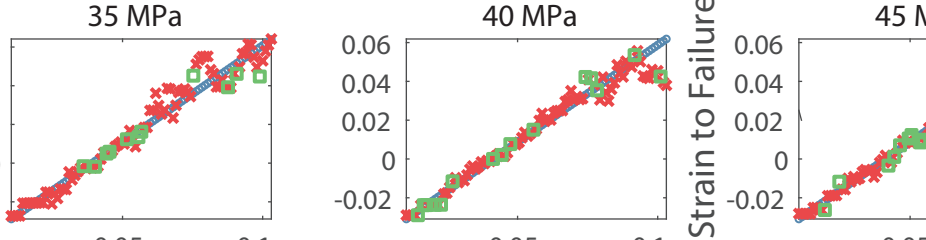
Blind Test:

Predict Stress-to-Failure for biaxial experiment at 25 MPa Confining



Blind Test:

Predict Strain-to-Failure for biaxial experiment at 25 MPa Confining



- Artificial Nerual Networks exhibit the capability to predict failure in Berea Sandstone using indicators of critical point behavior.
- Predictions of stress-to-failure and strain-to-failure improve as we approach critical point
- Uncertainty in predictions is larger in the Initiation and Frictional Sliding phases of the experiment.

Conclusions

- We conduct confined biaxial experiments on simulated samples of Berea Sandstone to analyze the time-space variation microcrack growth and associated energy release. We characterize distinct features prior to critical rock failure along heterogenous faults:
 - Increase in Microcracking Rate, Variance and Shear Microcrack Fraction
 - Increase in Fracture Energy Variance; Decline in Fracture Energy Kurtosis
 - Increase in Seismic Moment Range; Decline in seismic b-values
 - Decline in Fractal Distribution of Microcracks (D-value)
- The multivariate precursory analysis yields accurate predictions of stress-to-failure and strain-to-failure using Artificial Neural Networks.
 - Stress-to-Failure Prediction $R = 0.99$
 - Strain-to-Failure Prediction $R = 0.96$